



## Studying the complex BAL profiles in the BALQSOs spectra

**E. Lyratzi<sup>1,2</sup>, E. Danezis<sup>1</sup>, L. Č. Popović<sup>3</sup>, A. Antoniou<sup>1</sup>, M. S. Dimitrijević<sup>3</sup>, and D. Stathopoulos<sup>1</sup>**

<sup>1</sup> University of Athens, Faculty of Physics, Department of Astrophysics, Astronomy and Mechanics, Panepistimioupoli, Zographou 157 84, Athens, Greece,

<sup>2</sup> Eugenides Foundation, Syngrou 387, 175 64 P. Faliro, Greece

<sup>3</sup> Astronomical Observatory, Volgina 7, 11060 Belgrade, Serbia

elyratzi@phys.uoa.gr

**Abstract.** Most of Broad Absorption Lines (BALs) in quasars (QSOs) present very complex profiles. This means that we cannot fit them with a known physical distribution. An idea to explain these profiles is that the dynamical systems of Broad Line Regions (BLRs) are not homogeneous but consist of a number of density regions or ion populations with different physical parameters. Each one of these density regions gives us an independent classical absorption line. If the regions that give rise to such lines rotate with large velocities and move radially with small velocities, the produced lines have large widths and small shifts. As a result they are blended among themselves as well as with the main spectral line and thus they are not discrete. Based on this idea we study the BALs of UV C IV resonance lines in the spectra of a group of Hi ionization Broad Absorption Line Quasars (Hi BALQSOs) using the Gauss-Rotation model (GR model).

### 1. Introduction

Approximately about 10% of all quasars present broad, blue shifted absorption lines. The outflow velocity can reach up to 0.1–0.2  $c$ . Usually, in their spectra we observe the lines of high ionization species, as C IV  $\lambda$  1549 Å, Si IV  $\lambda$  1397 Å, N V  $\lambda$  1240 Å and Ly $\alpha$ . Rarely, some low ionization lines, such as Mg II  $\lambda$  2798 Å and Al III  $\lambda$  1857 Å, also exhibit broad absorption lines [see e.g. 1, 2]. Broad Absorption Lines (BALs) can have different shapes. Also different types of these objects may have differences in their continua [3].

One proposed explanation of the Broad Absorption Line (BAL) phenomenon is that BALQSOs (Broad Absorption Line Quasars) and non-BALQSOs are distinct populations of objects [4]. Similarly, some have argued that only low-ionization BALQSOs (LoBALs) are a different class of quasars [5].

Others suggest that BALQSOs and non-BALQSOs are the same type of quasar but viewed from different orientations [6–8] or at different stages in their life cycles [9].

The spectrum of a BALQSO is usually interpreted as a combination of (i) a broadband continuum arising from the central engine, (ii) the broad emission lines coming from the Broad Emission Line Regions (BELR), emerging near the center of the QSO and (iii) the broad absorption lines that are superposed, originating in a separate outlying region, so called Broad Absorption Line Region



(BALR) (see also [10]). However, it is also possible, that emission and absorption occur in the same line-forming region [11].

An important question is: Which are the physical connections between the BLR (Broad Line Region) and BALR? This is also important, since at least a part of the BLR seems to originate from wind of accretion disk [see 12, 13].

Another question is: Where is the BALR placed with respect to the center of a BALQSO and the BLR? To answer this question, one should investigate the kinematical properties of the emission and absorption lines.

Disk wind models [12, 14, 15] explain many properties of BAL quasars, but it is unclear if they can explain the full range of BAL profiles and column densities. BALs are caused by outflowing gas intrinsic to the quasar and are not produced by galaxies along the line of sight (as is the case for most narrow-absorption systems).

Determining whether a quasar is a BALQSO is a complicated task. The standard method is to calculate the “balmicity” index (BI), defined by Weymann et al. in [6]. A BI of zero indicates that broad absorption is absent, while a positive BI indicates not only the presence of one or more broad absorption lines but also the amount of absorption. The BI is essentially a modified equivalent width of the broad absorption line, expressed in velocity units and is defined as follows: (i) absorption should appear between 3000 and 25000 km/s blueward of C IV emission redshift and (ii) at this place and for at least 2000 km/s the absorption must fall at least 10% below the continuum. BIs can range from 0 to 20000 km/s.

We can classify the QSOs using the BI criterion in the following categories [16]:

- HiBALs: BALQSOs that present broad absorption trough just blueward of C IV emission.
- LoBALs: BALQSOs that present broad absorption troughs just blueward of both the C IV and Mg II emission lines.
- Non-BALs: BALQSOs that present no broad absorption troughs just blueward of the C IV and Mg II emission lines.
- FeLoBALs: BALQSOs with excited iron absorption features.

The 25000 km/s limit for the BI is chosen to avoid emission and absorption from Si IV. Absorption lines within 3000 km/s with width smaller than 2000 km/s are excluded to avoid contamination from absorption that might not be due to an outflow. These lines are called “associated absorption lines” [17]. Some of these associated systems are known to be intrinsic outflows, but others may simply be the result of absorption in the host galaxy or a nearby galaxy.

Here, we present some ideas in order to explain the complex structure of BALs in QSOs and especially we study the BALs of UV C IV resonance lines in the spectra of a group of Hi BALQSOs using the Gauss-Rotation model (GR model).

## 2. The multi-structure of BALs in QSOs

Most of BALs in QSOs present very complex profiles. This means that we cannot fit them with a known physical distribution. An idea is that the dynamical systems of BLRs are not homogeneous but consist of a number of density regions or ion populations with different physical parameters.

Each one of these density regions gives us an independent classical absorption line. If the regions that give rise to such lines rotate with large velocities and move radially with small velocities, the produced lines have large widths and small shifts. As a result they are blended among themselves as well as with the main spectral line and thus they are not discrete. A similar phenomenon can explain the very complex profiles of a great number of very broad lines in the spectra of hot emission stars [10, 18, 19].

Based on this idea we study the BALs of UV C IV resonance lines in the spectra of a group of Hi BALQSOs using the GR model [10, 18, 19].

The proposed model is relatively simple, aiming to describe the regions where the spectral lines are created. We assume that the BALR and BELR are composed of a number of successive independent absorbing/emitting density layers of matter (that originate in a disk wind). The absorbing regions have



three apparent velocities (projected on the line-of-sight of an observer): radial velocity ( $V_{\text{rad}}$ ) of the BALR, random velocity of the ions ( $V_{\text{rand}}$ ) in the BALR and the rotational velocity ( $V_{\text{rot}}$ ) of the BALR.

### 3. Data

In order to study the C IV resonance lines ( $\lambda\lambda$  1548.187, 1550.772 Å) we apply the GR model to the spectra of 15 Broad Absorption Line Quasars (BALQSOs) taken from the Sloan Digital Sky Survey’s Data Release 7. The SDSS imaging survey uses a wide-field multi-CCD camera [20]. The spectra cover the optical range 3800–9200 Å at a resolution of 1800–2100.

In table 1, column 1 lists the name of the QSOs, using the SDSS format of J2000.0 right ascension (hhmmss.ss) and declination ( $\pm$ ddmmss.s), column 2 lists the modified Julian date-plate-fiber, column 3 lists the redshift and column 4 lists the dates of observations.

**Table 1.** Studied BALQSOs

Object Name (SDSS)	MJD-Plate-Fiber	Redshift	Date
<b>J015024.44+004432.99</b>	51793-0402-485	2.00596	9/6/2000, 10:06
<b>J015048.83+004126.29</b>	51793-0402-505	3.70225	9/6/2000, 10:06
<b>J021327.25-001446.92</b>	51816-0405-197	2.39948	9/29/2000, 9:57
<b>J023252.80-001351.17</b>	51820-0407-158	2.03289	10/3/2000, 9:41
<b>J023908.99-002121.42</b>	51821-0408-179	3.74	10/4/2000, 9:38
<b>J025331.93+001624.79</b>	51816-0410-391	1.8214	9/24/2000, 11:26
<b>J025747.75-000502.91</b>	51816-0410-117	2.19139	9/24/2000, 11:26
<b>J031828.91-001523.17</b>	51929-0413-170	1.98447	1/20/2001, 4:23
<b>J102517.58+003422.17</b>	51941-0272-501	1.88842	2/1/2001, 9:30
<b>J104109.86+001051.76</b>	51913-0274-482	2.25924	1/4/2001, 11:00
<b>J104152.62-001102.18</b>	51913-0274-159	1.70876	1/4/2001, 11:00
<b>J104841.03+000042.81</b>	51909-0276-310	2.03044	12/31/2000, 11:08
<b>J110041.20+003631.98</b>	51908-0277-437	2.01143	12/30/2000, 11:19
<b>J110736.68+000329.60</b>	51900-0278-271	1.74162	12/22/2000, 12:12
<b>J112602.81+003418.23</b>	51614-0281-432	1.7819	3/11/2000, 6:52

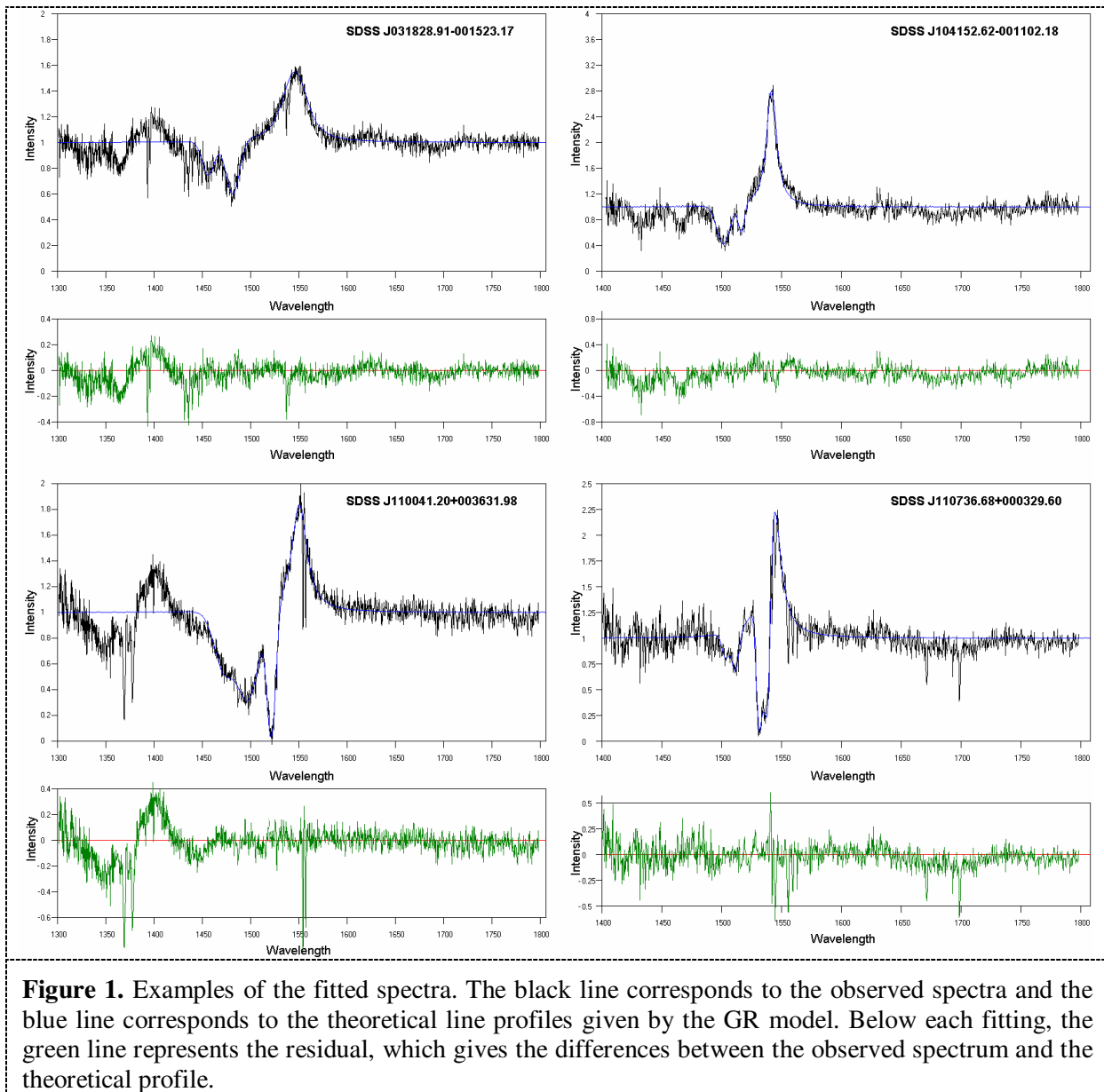
### 4. Method

The relevant broadening mechanism, in the case of BALs, is the random motion of the absorbing gas, but also a part comes from the rotation caused by the massive black hole. In order to find the limits for the rotational and random velocities, we fitted the observed lines using two approaches:

1. Gauss-Rotation approach (GR approach): We assume that random motion is dominant, i.e. the random velocity is maximal and the rotational component is minimal,
2. Rotation-Gauss approach (RG approach): We assume that the rotational component is dominant.

After that we used F-test to conclude on which approach of the model is more appropriate to explain the complex absorption line profiles.

In figure 1 we give some examples of the fitted spectra. The black line corresponds to the observed spectra and the blue line corresponds to the theoretical line profiles given by the GR model. Below each fitting, the green line represents the residual, which gives the differences between the observed spectrum and the theoretical profile.



## 5. Results

Using the GR model, we were able to fit the studied C IV spectral lines with 2 up to 4 absorption components and we calculated the values of the kinematical parameters (rotational, radial and random velocities), as well as the column density and the absorbed energy. The calculated values are given in tables 2-5. As one can see in tables 2-5, the radial velocity of the studied BALRs takes values between -2225 km/s and -17994 km/s, the values of the rotational velocity of the BALRs are between 30 km/s and 2400 km/s and the random velocity of the ions take values between 228 km/s and 2280 km/s. In most cases, the best fit of the observed spectral features is given by the GR approach. However, there were 4 cases (indicated with italics in tables 2-5), where the best fit is accomplished with the RG approach.



**Table 2.** Radial Velocities (km/s)

Object Name (SDSS)	Vrad <sub>1</sub>	Vrad <sub>2</sub>	Vrad <sub>3</sub>	Vrad <sub>4</sub>
J015024.44+004432.99	-3483	-7546		
J015048.83+004126.29	-3473	-5611		
J021327.25-001446.92	-3096	-5321		
J023252.80-001351.17	-5224	-8649		
J023908.99-002121.42	-8513			
J025331.93+001624.79	-4257	-5611		
J025747.75-000502.91	-7352			
J031828.91-001523.17	-13157	-17994		
<i>J102517.58+003422.17</i>	<i>-6772</i>	<i>-8126</i>	<i>-10545</i>	
J104109.86+001051.76	-2225	-5417	-6675	-9867
J104152.62-001102.18	-6385	-9287		
<i>J104841.03+000042.81</i>	<i>-5998</i>	<i>-8320</i>	<i>-11609</i>	
<i>J110041.20+003631.98</i>	<i>-5417</i>	<i>-10061</i>	<i>-14704</i>	
<i>J110736.68+000329.60</i>	<i>-2360</i>	<i>-3618</i>	<i>-7352</i>	<i>-8900</i>
J112602.81+003418.23	-6288	-7642		

**Table 3.** Rotational and Random Velocities (km/s)

Object Name (SDSS)	Rotational Velocities				Random Velocities			
	Vrot <sub>1</sub>	Vrot <sub>2</sub>	Vrot <sub>3</sub>	Vrot <sub>4</sub>	Vrand <sub>1</sub>	Vrand <sub>2</sub>	Vrand <sub>3</sub>	Vrand <sub>4</sub>
J015024.44+004432.99	2200	1500			1140	1368		
J015048.83+004126.29	500	200			456	228		
J021327.25-001446.92	100	100			935	912		
J023252.80-001351.17	100	1800			388	388		
J023908.99-002121.42	30				2280			
J025331.93+001624.79	250	200			570	410		
J025747.75-000502.91	1000				2052			
J031828.91-001523.17	350	150			1482	1368		
<i>J102517.58+003422.17</i>	<i>800</i>	<i>750</i>	<i>100</i>		<i>228</i>	<i>228</i>	<i>342</i>	
J104109.86+001051.76	200	50	50	100	342	342	570	798
J104152.62-001102.18	50	50			456	1140		
<i>J104841.03+000042.81</i>	<i>1000</i>	<i>500</i>	<i>500</i>		<i>388</i>	<i>410</i>	<i>456</i>	
<i>J110041.20+003631.98</i>	<i>1200</i>	<i>2400</i>	<i>1500</i>		<i>456</i>	<i>1482</i>	<i>2052</i>	
<i>J110736.68+000329.60</i>	<i>900</i>	<i>300</i>	<i>500</i>	<i>600</i>	<i>228</i>	<i>251</i>	<i>342</i>	<i>360</i>
J112602.81+003418.23	50	50			502	502		



**Table 4.** Column Density ( $\times 10^{10} \text{ cm}^{-2}$ )

Object Name (SDSS)	$\lambda 1548.187 \text{ \AA}$				$\lambda 1550.772 \text{ \AA}$			
	CD <sub>1</sub>	CD <sub>2</sub>	CD <sub>3</sub>	CD <sub>4</sub>	CD <sub>1</sub>	CD <sub>2</sub>	CD <sub>3</sub>	CD <sub>4</sub>
J015024.44+004432.99	-8.81	-3.51			-8.15	-3.20		
J015048.83+004126.29	-2.29	-0.78			-2.11	-0.71		
J021327.25-001446.92	-4.12	-2.03			-3.80	-1.85		
J023252.80-001351.17	-3.11	-3.67			-2.95	-3.38		
J023908.99-002121.42	-7.67				-7.04			
J025331.93+001624.79	-1.31	-0.87			-1.19	-0.80		
J025747.75-000502.91	-6.43				-5.90			
J031828.91-001523.17	-2.45	-1.39			-2.23	-1.26		
<i>J102517.58+003422.17</i>	<i>-1.82</i>	<i>-2.04</i>	<i>-0.51</i>		<i>-1.68</i>	<i>-1.89</i>	<i>-0.46</i>	
J104109.86+001051.76	-2.12	-1.58	-2.00	-2.81	-1.98	-1.46	-1.84	-2.58
J104152.62-001102.18	-0.94	-2.72			-0.85	-2.48		
<i>J104841.03+000042.81</i>	<i>-2.56</i>	<i>-1.73</i>	<i>-0.72</i>		<i>-2.36</i>	<i>-1.59</i>	<i>-0.66</i>	
<i>J110041.20+003631.98</i>	<i>-3.80</i>	<i>-5.65</i>	<i>-4.04</i>		<i>-3.51</i>	<i>-5.18</i>	<i>-3.68</i>	
<i>J110736.68+000329.60</i>	<i>-3.46</i>	<i>-1.87</i>	<i>-0.78</i>	<i>-0.53</i>	<i>-3.23</i>	<i>-1.74</i>	<i>-0.71</i>	<i>-0.48</i>
J112602.81+003418.23	-1.52	-2.21			-1.39	-2.04		

**Table 5.** Absorbed Energy (eV)

Object Name (SDSS)	$\lambda 1548.187 \text{ \AA}$				$\lambda 1550.772 \text{ \AA}$			
	Ea <sub>1</sub>	Ea <sub>2</sub>	Ea <sub>3</sub>	Ea <sub>4</sub>	Ea <sub>1</sub>	Ea <sub>2</sub>	Ea <sub>3</sub>	Ea <sub>4</sub>
J015024.44+004432.99	-13.55	-5.40			-12.53	-4.91		
J015048.83+004126.29	-3.52	-1.19			-3.25	-1.09		
J021327.25-001446.92	-6.34	-3.12			-5.85	-2.84		
J023252.80-001351.17	-4.78	-5.65			-4.53	-5.19		
J023908.99-002121.42	-11.81				-10.82			
J025331.93+001624.79	-2.01	-1.34			-1.83	-1.22		
J025747.75-000502.91	-9.90				-9.06			
J031828.91-001523.17	-3.77	-2.14			-3.42	-1.94		
<i>J102517.58+003422.17</i>	<i>-2.80</i>	<i>-3.14</i>	<i>-0.78</i>		<i>-2.57</i>	<i>-2.90</i>	<i>-0.70</i>	
J104109.86+001051.76	-3.27	-2.43	-3.08	-4.32	-3.04	-2.24	-2.83	-3.96
J104152.62-001102.18	-1.44	-4.19			-1.31	-3.81		
<i>J104841.03+000042.81</i>	<i>-3.94</i>	<i>-2.67</i>	<i>-1.11</i>		<i>-3.62</i>	<i>-2.45</i>	<i>-1.01</i>	
<i>J110041.20+003631.98</i>	<i>-5.84</i>	<i>-8.70</i>	<i>-6.21</i>		<i>-5.40</i>	<i>-7.95</i>	<i>-5.65</i>	
<i>J110736.68+000329.60</i>	<i>-5.32</i>	<i>-2.87</i>	<i>-1.20</i>	<i>-0.81</i>	<i>-4.97</i>	<i>-2.68</i>	<i>-1.09</i>	<i>-0.73</i>
J112602.81+003418.23	-2.33	-3.40			-2.13	-3.14		



## 6. Final remarks

The main purpose of this study is to answer to the question: Is a multi-structure of BLR regions able to explain the complex profile of Hi BALQSOs spectra?

Additionally, if the answer of the above question is positive, our next step is to test whether the GR model is able to reproduce the complex profiles of Hi BALQSOs and to calculate a group of physical parameters of the corresponding BLRs.

Concluding the results of our study we could remark that:

1. It is possible that the dynamical systems of BLRs are not homogeneous but consist of a number of density regions or ion populations with different physical parameters. Each one of these density regions gives us an independent classical absorption line. If the regions that give rise to such lines rotate with large velocities and move radially with small velocities, the produced lines have large widths and small shifts. As a result they are blended among themselves as well as with the main spectral line and thus they are not discrete.
2. As we can see in tables 2-5, the GR model is able to reproduce accurately the complex profiles of Hi BALQSOs and to calculate a group of physical parameters of the corresponding BALRs.

## Acknowledgements

This research project is progressing at the University of Athens, Department of Astrophysics, Astronomy and Mechanics, under the financial support of the Special Account for Research Grants, which we thank very much. This work also was supported by Ministry of Science Technological Development of Serbia and, through the projects “Influence of collisional processes on astrophysical plasma line shapes” and “Astrophysical spectroscopy of extragalactic objects”.

Funding for the SDSS and SDSS-II has been provided by the Alfred P. Sloan Foundation, the Participating Institutions, the National Science Foundation, the U.S. Department of Energy, the National Aeronautics and Space Administration, the Japanese Monbukagakusho, the Max Planck Society, and the Higher Education Funding Council for England. The SDSS Web Site is <http://www.sdss.org/>.

The SDSS is managed by the Astrophysical Research Consortium for the Participating Institutions. The Participating Institutions are the American Museum of Natural History, Astrophysical Institute Potsdam, University of Basel, University of Cambridge, Case Western Reserve University, University of Chicago, Drexel University, Fermilab, the Institute for Advanced Study, the Japan Participation Group, Johns Hopkins University, the Joint Institute for Nuclear Astrophysics, the Kavli Institute for Particle Astrophysics and Cosmology, the Korean Scientist Group, the Chinese Academy of Sciences (LAMOST), Los Alamos National Laboratory, the Max-Planck-Institute for Astronomy (MPIA), the Max-Planck-Institute for Astrophysics (MPA), New Mexico State University, Ohio State University, University of Pittsburgh, University of Portsmouth, Princeton University, the United States Naval Observatory, and the University of Washington.

## References

- [1] Hamann F, Korista K T and Morris S L 1993 *ApJ* **415** 541
- [2] Crenshaw M D, Kraemer S B and George I M 2003 *ARAA* **41** 117
- [3] Reichard T A, Richards G T, Hall P B, Schneider D P, Vanden Berk D E, Fan X, York Donald G, Knapp G R and Brinkmann J 2003 *AJ* **126** 2594
- [4] Surdej J and Hutsemekers D 1987 *A&A* **177** 42
- [5] Boroson T A and Meyers K A 1992 *ApJ* **397** 442
- [6] Weymann R J, Morris S L, Foltz C B and Hewett P C 1991 *ApJ* **373** 23
- [7] Ogle P M, Cohen M H, Miller J S, Tran H D, Goodrich R W and Martel A R 1999 *ApJS* **125** 1
- [8] Schmidt G D and Hines D C 1999 *ApJ* **512** 125
- [9] Becker R H, White R L, Gregg M D, Brotherton M S, Laurent-Muehleisen S A and Arav N 2000 *ApJ* **538** 72
- [10] Lyrtzi E, Popović L-Č, Danezis E, Dimitrijević M S, Antoniou A 2009 *NewAR* **53** 179



- [11] Branch D, Leighly K M, Thomas R C and Baron E 2002 *ApJL* **578** L37
- [12] Murray N and Chiang J 1998 *ApJ* **494** 125
- [13] Popović L-Č, Mediavilla E, Bon E, Ilić D 2004 *A&A* **423** 909
- [14] Proga D, Stone J M and Kallman T R 2000 *ApJ* **543** 686
- [15] Williams R J R, Baker A C, Perry J J 1999 *MNRAS* **310** 913
- [16] Richards G T et al. 2001 *AJ* **121** 2308
- [17] Foltz C B, Weymann R J, Peterson B M, Sun L, Malkan M A and Chaffee F H 1986 *ApJ* **307** 504
- [18] Danezis E, Popović L-Č, Lyratzi E and Dimitrijević M S 2006 *AIP Conference Proceedings* **876** 373
- [19] Danezis E, Nikolaidis D, Lyratzi E, Popović L-Č, Dimitrijević M S, Antoniou A and Theodosiou E 2007 *PASJ* **59** 827
- [20] Gunn J E et al. 1998 *AJ* **116** 3040